A survey of test methods for multiaxial and out-of-plane strength of composite laminates

Robin Olsson

Review

A survey of test methods for multiaxial and out-of-plane strength of composite laminates

Robin Olsson

PII: S0266-3538(11)00050-9
DOI: 10.1016/j.compscitech.2011.01.022
Reference: CSTE 4917

To appear in: *Composites Science and Technology*

Received Date: 15 September 2010
Revised Date: 24 January 2011
Accepted Date: 30 January 2011

Please cite this article as: Olsson, R., A survey of test methods for multiaxial and out-of-plane strength of composite laminates, *Composites Science and Technology* (2011), doi: 10.1016/j.compscitech.2011.01.022

Revision 1 submitted to Composites Science and Technology by Robin Olsson 24 Jan. 2011

A survey of test methods for multiaxial and out-of-plane strength of composite laminates

*Robin Olsson**

Swerea SICOMP AB, Box 104, SE-431 22 Mölndal, Sweden

Abstract

This review paper gives an overview of test methods for multiaxial and out-of-plane strength of composite laminates, with special consideration of non-crimp fabrics (NCF) and other textile systems. Tubular and cruciform specimens can provide arbitrary in-plane loading, while off-axis and angle-ply specimens provide specific biaxial loadings. Tensile and compressive out-of-plane strength may be determined by axial loading of specimens with a waisted gauge section, while bending of curved specimens allow determination of the out-of-plane tensile strength. Tests suited for out-of-plane shear strength include the short beam shear test, the inclined double notch test and the inclined waisted specimen. Testing of arbitrary tri-axial stress states using tubular or cruciform specimens with superimposed through-the-thickness loading is highly complex and significant problems have been reported in achieving the intended stress states and failure modes. Specific tri-axial stress states can be obtained by uniaxial loading of specimens with constrained expansion, as in the die channel test.

Keywords

A: Polymer-matrix composites (PMCs), Structural composites, Textile composites

B: Strength D: Multiaxial testing

*) Corresponding author. *Tel:* +46-31-706 63 51. *E-mail:* robin.olsson@swerea.se

1. Introduction

High performance fibre composites are used extensively in the aerospace sector, where they traditionally have been used in relatively thin laminates made from prepreg material. The stresses in such structures are typically dominated by in-plane loads and stresses, Figure 1a, although failure sometimes occurs due to large local out-of-plane stresses at flange-web transitions, Figure 1b.

Growing confidence in composite materials and new and cheaper manufacturing methods based on resin infusion of dry fibre preforms, e.g. Non-Crimp Fabrics (NCF), have resulted in increasing use of composites in components with more complex geometry and loading, and a correspondingly more complex stress state, Figure 1c. Examples of aircraft components with complex shape where composite materials are considered or are being used include guide vanes and fan blades for aeroengines, spars for wings, and window/door frames for the fuselage.

Figure 1 Transition from fully two-dimensional (a) to fully three-dimensional (c) stress states

This development necessitates three-dimensional (3D) failure criteria and tests to determine strength data for accompanying out-of-plane and multiaxial loading. A general overview of available 3D failure criteria, with focus on composite materials, was given in [1].

Composites generally have an inhomogeneous microstructure, e.g. involving fibres and matrix, while the macrostructure usually is considered homogeneous. Conventional unidirectional tape prepreg systems tend to have a homogenous structure also at the meso-scale (ply level). In contrast, composites with textile fibre architecture, e.g. NCF

materials, are inhomogeneous at the meso-scale, which involves fibre bundles and resin rich pockets.

The out-of-plane strength of these new thick composite materials with a complex meso-structure must clearly be considered, particularly as it usually is significantly lower than the in-plane strength. Due to the previous focus on thin laminates under primarily in-plane loads the tests for strength under out-of-plane and triaxial loads are not well developed and the experience of using them is small, particularly in the industry. This limitation has been tolerable for traditional unidirectional (UD) prepreg systems, which often can be approximated as transversely isotropic perpendicular to the fibres. In contrast, NCF systems and other textile fibre architectures result in an orthotropic material on the mesoscale (ply level), where dedicated out-of-plane tests are necessary for a correct material description.

The aim of this review is to give an overview of available test methods for the strength and stiffness of composite laminates under uniaxial and multiaxial out-of-plane loading. It should be stressed that the current paper does not aim to provide an exhaustive review, but rather to illustrate approaches by a selection of available test methods and to highlight problems associated with the various methods.

2. Biaxial in-plane testing

"Multiaxial" and biaxial testing of composites was reviewed in [2], but a careful examination of the paper clarifies that "multiaxial" solely refers to various combinations of in-plane loads. Furthermore it should be recognised that since the publication of the review a fair amount of additional research has been done in the area. Biaxial test

methods, with particular focus on issues with tubular specimens, have also been discussed in a review of biaxial failure criteria for polymer composites [3].

2.1 Tubular specimens

Tubular specimens are the obvious choice for material systems which normally are used in cylindrical components, e.g. components made by filament winding. They may also be suitable for testing of prepreg materials used in flat laminates, provided that sufficiently similar fibre volume fractions, meso-scale architecture and void contents can be achieved. The main advantage of tubular specimens is the absence of free edge effects. Main difficulties are more complex manufacturing and difficulties in controlling the manufacturing quality.

Unidirectional 90º ply cylindrical specimens under combined twisting and axial tension or compression, Figure 2a, have been used to test matrix-controlled biaxial failure, e.g. in [4].

Arbitrary biaxial in-plane loading of laminates may be obtained by internally pressurised tubular specimens under combined twisting and tension or compression, Figure 2b. Such specimens have been extensively studied by Swanson and co-workers, and a review of this work was presented in [5]. Additional work using the same approach has been presented e.g. in [6].

Figure 2 Tubular specimens for (a) transverse normal/shear and (b) arbitrary biaxial loads [5] © Elsevier. Reproduced with permission.

A common assumption in the analysis of internally pressurised tubes is that a plane stress analysis is applicable. For thin walled tubes this assumption is certainly satisfied

when comparing the out-of-plane (radial) stress with the average in-plane stress over the thickness. In a multi-directional laminate the local in-plane ply stresses transverse to the fibres are, however, significantly smaller than the average in-plane stress. Thus, the stress state of the inner plies will be more or less three-dimensional, while the outer plies will be in a purely plane stress state. It is likely that the out-of-plane compressive stress will delay failure of the inner plies, so that failure initiates at the outside of the tube.

2.2 Cruciform specimens

Cruciform composite specimens have been developed using previous experience with similar metal specimens, and a correct design may allow testing under more or less arbitrary biaxial (in-plane) loads. Examples of their design and application to composites may be found in a paper by Welsh & Adams [7], who also review their extensive previous work in this area. A more recent study of cruciform composite specimens involving full field optical measurements was published in [8], which provided an extensive review of previous work.

A major advantage of cruciform specimens is that they are representative for the material in existing flat laminates and comparatively easy to manufacture, although specimens often become relatively large and require extensive machining. Complicating factors are the needs for machining of a reduced thickness in the gauge section and a corner fillet, Figure 3, which are required to prevent premature failure outside the gauge section.

Figure 3 Typical cruciform specimen with reduced thickness gauge section

Compiled from [7] © Elsevier. Reproduced with permission.

Test machines for biaxial cruciform specimens are inherently complex. A minimum of two separate and orthogonal actuators are generally required. As pointed out in [8] the preferred option is four separate actuators, Figure 4a, and a control system with an appropriate feed back loop since only two actuators will lead to asymmetric deformation of the specimen, Figure 4b.

Figure 4 Cruciform specimen with four actuators (a) two actuators (b). [8] © Elsevier. Reproduced with permission

2.3 Specimens giving specific biaxial loads

2.3.1 Off-axis specimens

Axial loading of unidirectional coupons with the fibres at an angle to the loading direction can provide a certain range of biaxial stress states. The failure strains in various directions of a composite are usually of the same order, while the stiffness, and hence strength, varies by an order of magnitude. For this reason it is more convenient to compare strain ratios than stress ratios. Figure 5 shows the resulting strain ratios in the local (material) coordinate system for axial loading at different off-axis angles of typical carbon (CFRP) and glass (GFRP) reinforced unidirectional specimens. Note that Figure 5 uses the absolute value of γ_{12}.

Figure 5 Strain states for axial loading of UD off-axis specimens

It is evident that significant strains in the fibre direction can only be achieved for loading entirely along the fibres or in combination with relatively large shear strains, which are likely to control the failure. On the other hand off-axis angles between 30º

and 90º allow virtually arbitrary combinations of shear strain and transverse normal strain, with negligible strain in the fibre direction. At an off-axis angle of about 8º for CFRP and 15º for GFRP, the transverse normal strain ε_2 is zero, while the shear strain is about 3-4 times the strain in the fibre direction. For this reason 10º off-axis specimens have been examined as a candidate for testing in-plane shear strength [9-10].

A major problem with off-axis specimens is the deformation incompatibility at the loading clamps, which inevitably causes premature failure. This problem may be significantly alleviated by use of end tabs cut at an oblique angle, equivalent to the iso-displacement lines of the specimen [11]. The angle ϕ between these lines and the loading axis of the specimen is given by:

$$\cot\phi = -S_{16}/S_{11} \tag{1}$$

where $S_{ij}=A_{ij}^{-1}$ are components of the compliance matrix of the laminate.

2.3.2 Angle-ply specimens

Axial loading of angle-ply coupons with the fibres in alternating angles to the loading direction can provide a certain range of biaxial stress states. Figure 6 shows the resulting strain ratios in the local (material) coordinate system for axial loading at different off-axis angles of typical carbon (CFRP) and glass (GFRP) reinforced unidirectional specimens. The strain states that can be achieved seem to be similar as for the off-axis specimens. At a ply angle of about 43º for CFRP and 39º for GFRP, the transverse normal strain ε_2 is zero, while the shear strain is much higher (about 13 times for CFRP and 5 times for GFRP) than the strain in the fibre direction. For this reason

±45º angle ply specimens have been widely used for testing of in-situ in-plane shear strength.

Figure 6 Strain states for axial loading of angle-ply specimens

2.3.3 Biaxial in-plane Arcan test

The Arcan test was originally developed for shear testing of polymers and composites. By adding a sequence of loading holes, Figure 7a, it is possible to achieve arbitrary combinations of shear and tension transverse to the fibres [12]. A recent study of biaxial tensile-shear testing indicated somewhat higher strength than in conventional off-axis tests [13]. Combined shear and compression is possible to achieve by addition of a fairly complex supporting rig as shown in Figure 7b [14].

Figure 7 Biaxial Arcan test with transverse stress in (a) tension and (b) compression [14] © SAMPE International. Reproduced with permission.

2.3.4 In-plane shear and normal stress with dual actuators

In recent years two tests with independent dual actuators for combined inplane shear and normal stresses have been developed. Vogler & Kyriakides [15] studied how the strain rate under combined in-plane shear and compressive loading in the fibre direction influenced the yielding and failure of an AS4/PEEK composite, Figure 8a. In [16] the interaction between in-plane shearing and transverse tensile stresses on an NCF composite was studied using a similar device, Figure 8b.

Figure 8 Biaxial test with shear and transverse stress in (a) compression and (b) tension. (a): [15] and (b): [16]. Both © Elsevier. Reproduced with permission.

3. Uniaxial out-of-plane testing

3.1 Tensile and compressive testing

The two basic methods for interlaminar tensile/compressive testing include various versions of waisted coupons for axial loading, Figure 9a, and coupons achieving interlaminar tensile stresses through flexure of curved beams, Figure 9b [17].

Figure 9 Interlaminar tensile test by (a) axial loading (b) flexure. [17] © Elsevier. Reproduced with permission.

3.1.1 Axial loading

Axial loading, like that shown in Figure 9a, is straightforward, but requires that a number of conditions are satisfied while designing the specimen:

- Sufficient width to incorporate at least four representative volume elements of the material
- Sufficient height to width ratio to obtain uniaxial stresses in the gauge section
- Careful waisting to reduce stress concentrations and premature failure

The main drawback of these specimens is the relatively complicated manufacturing. Furthermore, specimens either have to be made from very thick laminates which normally have different microstructure and volume fractions than thin laminates, or

have to be manufactured by bonding several thin laminates on top of each other. The bond lines have a different strength and may cause artificially induced stress variations in the specimen.

Specimens of the type shown in Figure 9a have been tested for composites in [18], where several 3 mm laminates were bonded on top of each other to obtain a square gauge section. It was found that failure frequently occurred close to the bond lines, rather than within the composite material.

A similar specimen with rectangular gauge section was developed at DERA by Ferguson, Hinton and Hiley [19], Figure 10a. The geometry of this specimen was obtained through careful FE-analysis. A miniature (half scale) specimen was also developed and was found to provide similar results. The specimens were assessed in tensile and compressive tests on a wide range of fibre composites, including UD carbon/epoxy prepreg, glass/epoxy material manufactured through filament winding, press forming and RTM, as well as random short glass fibre systems involving various resins and manufacturing routes. Compression tests were uncomplicated, while the end tab extensions used in the tension tests (Figure 10b) were found to cause premature failure in some tensile tests due to difficulties with correct alignment.

Similar waisted specimens with 17 mm thickness and a square gauge section were developed in [20], where FE analysis also was used for improving the geometry. An interesting feature of these specimens was the use of thin epoxy end blocks, which reduced stress concentrations and had higher strength than the composite specimen.

Figure 10 *The DERA specimen for through-thickness testing: (a) geometry of standard size specimen, (b) comparison of tensile (tabbed) and compressive specimens. [19] © Elsevier. Reproduced with permission.*

A spool specimen was developed in [21]. The geometry is similar to the one shown in Figure 10, but the specimen cross sections are cylindrical rather than rectangular. Careful selection of the geometry limited the peak stress in the gauge section to 1.1 of the nominal stress for the quasi-isotropic layup employed in the spool specimens. In addition to static tests these authors performed fatigue tests and made detailed comparisons with a unidirectional layup in U-shaped specimens loaded in bending. It was shown that the somewhat lower strength in the U-shaped specimens could be explained by the larger stressed volume in these specimens. Furthermore, the strengths of both the spool specimens and the U-shaped specimens could be directly linked to the transverse strength in conventional in-plane tensile coupons through a Weibull scaling law, using expressions presented in [22].

3.1.2 Flexural loading

A number of specimens have been developed for using flexure to obtain an interlaminar tensile stress, and reviews of such tests have been given in [17] and [23]. Extensive work was done by Jackson and Martin [24], who developed an interlaminar tensile test using tensile loading of an L-shaped coupon, Figure 11a. A very similar specimen was presented in [25], and the only major difference appears to be that the moment arms have been extended by aluminium tabs. Subsequently a four-point bend version of the test by Jackson and Martin was developed in [26], Figure 11b. This version has been implemented in the test standard ASTM D6415. One advantage of the four-point bend configuration is that no axial load is superimposed in the specimen arms, but the influence on the specimen stress state is very minor, Figure 12. The main advantages of

the four-point bend test pointed out in [26] are the self-aligning specimen and the simplified specimen preparation and setup.

Figure 11 Interlaminar tensile tests: a) Hinged loading; b) 4-Point-bend loading .
[26] © ASTM International. Reproduced with permission.

Comparisons with FE analysis confirmed that the stress state in the specimen by Jackson & Martin [24] could be accurately described by modification of an elasticity solution by Lekhnitskii, and that the axial (in-plane) stress σ_θ in the curved section was zero in the critical interface with peak interlaminar (through-the-thickness) stress σ_r, Figure 12.

Figure 12 Stress distributions in the L-shaped flexural specimens.
[26] © ASTM International. Reproduced with permission.

Figure 13 gives a comparison of the interlaminar tensile strength obtained with the hinged and four-point bend versions of the L-shaped specimen for different prepreg tape and textile RTM systems. Similar fibre volume fractions were used and the prepreg resin 3501-6 was considered similar to the RTM resin RSL-1895/W, but the out-of-plane tensile strength of the textile systems was significantly lower than for the prepreg specimens. The strength of the textile systems was, however, relatively independent of fibre architecture and unit cell size and consistent results were obtained even for unit cell sizes less than the specimen width.

Figure 13 Out-of-plane tensile strength of different material systems.

[26] © ASTM International. Reproduced with permission.

The main conclusion from the tests in [24] was that the interlaminar tensile strength was highly dependent on the laminate quality and void content. The measured strength varied by a factor of four depending on geometrical factors of the specimen, such as thickness and radius of curvature at the bend, Figure 14.

Figure 14 Geometry influence on interlaminar tensile strength.

(σ_{2c} is in-plane tensile strength, σ_{3c} is out-of-plane tensile strength and r_i inner radius)

[24] © ASTM International. Reproduced with permission.

The decreasing strength was linked to an increasing ply thickness in the region under high radial stress (0.3-0.4 normalized radial distance, c.f. Figure 12). Figure 15 illustrates that the increasing ply thickness in this region could be linked to an increasing inner radius and thickness of the laminate. The increasing ply thickness was assumed to correspond to an increasing amount of porosity and defects, which was supported by microscopic observations. There is also a volumetric effect, which in Figure 14 is illustrated by differences in strength between the 16, 24 and 48 ply laminates and between 12.7 and 25.4 mm wide specimens. Similar effects have been observed in [21] and in [25]. In [26] it was demonstrated that the differences in strength between specimens of different width could be fully accounted for by using a Weibull volume scaling law, as suggested in [22].

Figure 15 Geometry influence on ply thickness.

(r is radial position, r_i inner radius and t laminate thickness, c.f. Fig. 11a)

[24] © ASTM International. Reproduced with permission.

It may be concluded that L-shaped specimens are not suitable for studying "perfect" materials, but could be very useful in testing the material properties associated with typical components where interlaminar failure is common, e.g. spar-web transitions etc.

3.2 Shear testing

From equilibrium considerations the through-thickness shear stresses are identical to the interlaminar shear stresses, and failure will obviously occur at the weakest plane. There are a number of tests which can be used to determine interlaminar shear strength, e.g. the Short 3 Point Bend (S3PB) test, the Iosipescu test, the V-Notched Rail Shear Test, the Double Notch Compression (DNC) test, the Inclined Double Notch Shear (IDNS) test and the Arcan specimen, Figure 16. ASTM test standards exist for the S3PB test (ASTM D2344), the Iosipescu test (ASTM D5379) and the V-Notched Rail Shear Test (ASTM D7078). A major disadvantage of all the shear tests mentioned is that the shear stresses are fairly nonuniformly distributed across the specimen gauge section. In most cases the high shear stresses are confined to a narrow band which necessitates use of relatively small shear strain gauges or optical strain measurements with high spatial resolution for determining the shear modulus.

Figure 16 Tests for interlaminar shear strength: a) Iosipescu test, b) Short 3 Point Bend test, c) Double Notch Compression test, d) Inclined Double Notch Shear test, e) Inclined waisted specimen, f) Arcan specimen.
Compiled from (a-d): [36] © ASTM. Reproduced with permission; (e): [20] © Maney Publishing. Reproduced with permission; (f): [13] © Elsevier. Reproduced with permission.

3.2.1 The Iosipescu test

The Iosipescu test (denoted V-notched beam method by ASTM), Figure 16a, has long been considered the most reliable test for shear strength, although the slightly nonuniform stress distribution in the gauge section means that the true shear strength of the material never is achieved. Issues related to the analysis of the specimen include effects of material and geometric nonlinearity [28-29]. Issues with geometrical imperfections, resulting in e.g. out-of-plane bending, have been considered e.g in [30] and [31]. A study of strain fields and material nonlinearity in a modified Iosipescu specimen was presented in [32].

There are significant differences in the strength obtained by testing the shear strength with fibres along or perpendicular to the notched gauge section, i.e. in the 90º or 0º directions, although these strengths should be equal for a linear elastic material. The differences have been explained by the fact that failure initiation with fibres in the 90º direction leads to more or less immediate failure, while fibres in the 0º direction allows significant damage growth and stress redistribution prior to ultimate failure [32].

A drawback of the Iosipescu test is that the required specimen height primarily makes it suited for testing the *intra*laminar shear strength. Sufficient specimen height for testing *inter*laminar shear strength can only be achieved by manufacturing very thick laminates or by bonding a large number of thin specimens on top of each other. Rare examples of use for testing interlaminar shear properties may be found in [33] and [34]. The study in [33] compared intralaminar and interlaminar shear properties, and used bonded dummy layers of woven prepreg to achieve sufficient height of the specimens for interlaminar testing. The study in [34] focused on thick laminates and included a thorough analysis

of stresses, manufacturing and curing issues, as well as an extensive review of previous work on the Iosipescu specimen.

3.2.2 The Short 3 Point Bend test

The S3PB test, Figure 16b, is frequently used by the industry for quality control, but the results at best only give a qualitative measure of the interlaminar shear strength. The reason is the complex stress state in the specimen, which in addition to interlaminar shear stresses also involves contact stresses at the points of load introduction and flexural stresses increasing towards the top and bottom surface. For these reasons it is common to observe invalid failure modes due to local contact crushing or flexural failure. The data reduction is based on an assumed parabolic shear stress distribution, which is only achieved under elastic conditions and in a small part of the specimen length. The assumed ratio between peak stress and average shear stress is 1.5, which is based on elastic conditions, but any material softening results in a decreasing ratio. Thus, the shear strength may be overestimated by as much as 50%.

3.2.3 The Double Notch Compression test

The Double Notch Compression (DNC) test, Figure 16c, is associated with severe stress concentrations at the two notches and hence the interlaminar shear strength is severely underestimated for most unidirectional fibre composites.

3.2.4 The Inclined Double Notch Shear test

The Inclined Double Notch Shear (IDNS) test, Figure 16d, is ideally suited to test interlaminar shear strength, due to the use of a fairly thin specimen and a very uniform stress state in the gauge section. The uniform stress state is obtained by suppression of the stress concentrations in the traditional DNC test through two superimposed point

loads. Two versions of the IDNS test have been designed, one involving a compressive test rig [27] and one involving a tensile test rig [35]. The shear strength measured in the IDNS test is significantly higher than for a corresponding failure along fibres (90º specimen) in the Iosipescu tests, as illustrated by the examples in Table 1 [36]. Note that the definitions of fibre directions in [36] here have been reversed to agree with the definitions in ASTM D5379, where the 0º direction represents the length axis of the specimen and 90º represents the thickness direction. The higher shear strength of the Iosipescu tests with 0º fibres was explained by extensive damage growth and stress redistribution after failure initiation. The high apparent shear strength in the S3PB test was associated with the assumption of an elastic stress distribution and the resulting overestimation of the peak shear stress. In fact, significant softening was observed in all the specimens [36].

Table 1 Shear strengths from different tests. Data from [36].

3.2.5 Inclined waisted specimen

The waisted specimen, Figure 16e [20], was developed in an attempt to reduce stress concentrations in a conventional rail shear test of a rectangular test block. The resulting out-of-plane compressive stress was found to be beneficial for preventing premature failure. The experimental results did, however, indicate an impure stress state in the specimen and the thoroughly analysed IDNS test appears to be a more obvious candidate for testing interlaminar shear strength.

3.2.6 Arcan specimen

The Arcan specimen, Figure 16f, was originally proposed for shear testing of polymers but has later also been applied to composite materials. In [37] a comparison was made of both in-plane and out-of-plane shear properties of a unidirectional fibre composite. A thorough review of previous work on the specimen was also provided. One advantage of the test is a fairly uniform stress distribution in the test section but the uniformity depends on direction of fibres versus load axis.

3.3 Specimen manufacturing issues.

There are a number of practical problems associated with manufacturing of axially loaded through-the-thickness test specimens. The aim to get a uniform uniaxial stress state requires that the specimen is fairly long in the loading direction, which implies use of very thick laminates. Thick laminates usually have a higher void content and larger variation in fibre distribution than thin laminates, which frequently is reflected in a lower strength. Difficulties in achieving similar fibre fractions may also cause different strength and stiffness in thick and thin laminates. For thick laminates made by bonding several thin laminates on top of each other it is not uncommon that the specimens fail close to the bond line so that the measured strength is not representative of the material in the original laminate. The problem of thick specimens is further aggravated for textile composites, due to the need to include a sufficient number of unit cells over the specimen width, as an increased width requires a corresponding increase in laminate thickness to maintain a suitable constant length/width aspect ratio of the specimen.

4. Triaxial testing

4.1 Tubular specimens

The in-plane and out-of-plane material stresses σ_1, σ_2, τ_{12} and σ_3 at failure of tubular specimens loaded by combined internal pressure, axial tension or compression and axial torsion were presented in [6]. It should, however, be noted that the out-of-plane stress σ_3 varies between a peak (negative) value at the inside of the pipe to zero at the outside, and that the reported stress σ_3 is just the interior peak stress. Thus, these tests do not represent a uniform triaxial stress state and are essentially comparable to the tests in [5], where the tests were reported as biaxial.

4.2 Cruciform specimens

Triaxial loading of flat cruciform specimens has been considered by adding an additional set of load actuators in the specimen thickness direction. The design of such a test facility has been described in [38], where cylindrical steel attachments were used to apply the load in the thickness direction of the gauge section. Experimental tests involving various combinations of tensile and compressive in-plane and out-of-plane loads on cross-ply laminates have been described in [39]. The out-of-plane compressive strength was found to be virtually insensitive to the in-plane loads, possibly due to the cross-ply layup which severely constrained the in-plane strains. The measurement of the out-of-plane tensile strength in combination with in-plane loads was unsuccessful, as the bonding of the out-of-plane load attachments to the gauge section failed prematurely.

4.3 Specimens giving specific triaxial loads

There appears to be a lack of standardised specimens providing specific uniform triaxial stress states. Complex specimen geometries provide a range of triaxial stress stresses, but the drawback of such specimens is the nonuniform stress state, which makes it difficult to study failure under a specified stress state. Thus, the stress state at failure has to be deduced from a stress analysis for the observed location of failure.

4.3.1 Constrained out-of-plane compression

A simple specimen providing a uniform triaxial stress state is the "die channel test" with constrained compression of a rectangular block of orthotropic material, Figure 17. In the figure a transversely isotropic material is loaded in the plane of symmetry, while it is free to expand in the axial direction. If friction is neglected this produces biaxial stresses with an approximate ratio of 3:1 in the 2-3 plane. A triaxial stress state is obtained if the expansion is also constrained in the axial direction of the material.

Tests of the type shown in Figure 17 were performed on unidirectional CFRP in [40], where a transition was shown from a failure plane parallel to the fibres in unconstrained specimens to a failure plane cutting through the fibres (as indicated in the figure) in the constrained specimen. This resulted in an almost tenfold increase in compressive strength. Very similar effects have been observed in out-of-plane compression of cross-ply CFRP laminates [41].

Figure 17 Out-of-plane compression of constrained specimen

4.3.2 Biaxial out-of-plane Arcan test

By using the sequence of loading holes on the Arcan specimen, Figure 16f, it is possible to achieve arbitrary combinations of shear and tension transverse to the fibres. This approach was originally proposed for in-plane testing of composites[12] but can in principle also be applied to out-of-plane testing, although specimen manufacturing becomes more complicated.

5. Conclusions

Significant problems exist in determining the strength of composite laminates under arbitrary biaxial and triaxial loading. Available specimens are expensive to manufacture and the required test rigs complicated. Thus, such tests will find limited use in industry. The most realistic route appears to be to develop multiaxial failure criteria based on data from tests in uniaxial in-plane and out-of-plane loading and to validate the criteria on a few tests providing specific multiaxial stress states.

Tests for tensile and compressive strength under uniaxial out-of-plane loading are fairly straight-forward but relatively thick laminates are required. Out-of-plane tensile testing by flexural loading of curved specimens allows thinner laminates, but results from these specimens have indicated significant Weibull volume effects, and problems in obtaining a uniform material quality through the thickness.

The Iosipescu test and Inclined Double Notch Shear (IDNS) test appear to be the most appropriate tests for determination of shear strength, but only the IDNS test appears to be suitable for out-of-plane testing.

Specific biaxial and multiaxial stress states may be obtained by uniaxial loading of constrained specimens, but guidelines for design of such specimens are not readily

available. Further work is needed to design practical tests and specimens providing a sufficient range of stress ratios.

Testing of composites with textile fibre architectures presents particular problems, due to the need to include a sufficient number of representative volume elements, which may increase specimen thickness and other dimensions significantly.

6. Acknowledgements

This work is a part of the ReFACT project, which is funded by the Fifth Swedish National Aeronautical Research Programme (NFFP5).

7. References

[1] Marklund E (2010). Literature survey of 3D failure criteria. TR10-002. Swerea SICOMP AB, Piteå, Sweden.

[2] Chen AS, Matthews FL (1993). A review of multiaxial/biaxial loading tests for composite materials. Composites;24(5):395-406.

[3] Thom H (1998). A review of the biaxial strength of fibre-reinforced plastics. Composites Part A;29(8):869-886.

[4] Swanson SR, Messick MJ, Tian Z (1987). Failure of carbon/epoxy lamina under combined stress. J Compos Mater;21(7):619-630.

[5] Swanson SR, Qian Y (1992). Multiaxial characterization of T800/3900-2 carbon/epoxy composites. Compos Sci Technol;43(2):107-203.

[6] Cohen D (2002). Multi-axial tube test method. Composite materials: Testing, design, and acceptance criteria, ASTM STP1416. Eds: Zureick A, Nettles AT. ASTM:17-29.

[7] Welsh JS, Adams DF (2002). An experimental investigation of the biaxial strength of IM6/3501-6 carbon/epoxy cross-ply laminates using cruciform specimens. Composites Part A;33(6):829-839.

[8] Smits A, Van Hemelrijck D, Philippidis TP, Cardon A (2006). Design of a cruciform specimen for biaxial testing of fibre reinforced composite laminates. Compos Sci Technol;66(7-8):964-975.

[9] Chamis CC, Sinclair JH (1977). 10-deg off-axis test for shear properties in fiber composites. Exp Mech;17(9):339-346.

[10] Pierron F, Vautrin A (1996). The 10º off-axis tensile test: a critical approach. Compos Sci Technol;56(4):483-488.

[11] Sun CT, Chung I (1993). An oblique end-tab design for testing off-axis composite specimens. Composites;24(8):619-623.

[12] Voloshin A, Arcan M (1980). Failure of unidirectional fiber-reinforced materials – new methodology and results. Exp Mech;29(8):280-284.

[13] El-Hajjar R, Haj-Ali R (2004). In-plane shear testing of thick-section pultruded FRP composites using a modified Arcan fixture. Composites Part B;35(5):421-428.

[14] Van Den Broucke B, et al. (2007). Failure and impact modelling of textile composites: ITOOL project. In Proc. SAMPE Europe International Conference. Paris: 227-232.

[15] Vogler TJ, Kyriakides S (1999). Inelastic behaviour of an AS4/PEEK composite under combined transverse compression and shear. Part I: experiments. Int J Plasticity;15(8):783-806.

[16] Greve L, Bisagni C, Walters CL (2010). Biaxial experimental determination of in-plane matrix failure envelope of unidirectional composite. Composites Part A;41(6):750-758.

[17] Kedward KT, Wilson RS, McLean SK (1989). Flexure of simply curved composite shapes. Composites;20(6):527-536.

[18] Lagace, PA, Weems DB (1989). A through-the-thickness strength specimen for composites. In: Test methods for design allowables for fibrous composites, Second volume, ASTM STP1003, Ed: Chamis CC. ASTM, Philadelphia:197-207.

[19] Ferguson RF, Hinton MJ, Hiley MJ (1997). Determining the through-thickness properties of FRP materials. Compos Sci Techn;58(9):1411-1420.

[20] Mespoulet S, Hodgkinson JM, Matthews FL, Hitchings D, Robinson P (2000). Design, development and implementation of test methods for determination of through thickness properties of laminated composites. Plastics, Rubber and Composties;29(9):496-502. Online version: www.maney.co.uk/journals/prc or www.ingentaconnect.com/content/maney/prc.

[21] Koudela KL, Strait LH, Caiazzo AA, Gipple KL (1997). Static and fatigue interlaminar tensile characterization of laminated composites. In: Composite materials: Fatigue and fracture (Sixth volume), ASTM STP1285, Ed: Armanios EA. ASTM, Philadelphia:516-530.

[22] O'Brien TK, Salpekar SA (1993). Scale effects on the transverse tensile strength of graphite epoxy composites. In: Composite materials and design (Eleventh volume), ASTM STP1206, Ed: Camponeschi ET, Jr. ASTM, Philadelphia:23-52 (also NASA TM 107637. NASA LaRC, 1991).

[23] Cui W, Liu T, Len J, Ruo R (1996). Interlaminar tensile strength (ILTS) measurement of woven glass/polyester laminates using four-point curved beam specimen. Composites Part A;27A(11):1097-1105.

[24] Jackson WJ, Martin RH (1993). An interlaminar tensile strength specimen. In: Composite materials: Testing and design (Eleventh volume), ASTM STP1206, Ed: Camponeschi ET, Jr. ASTM, Philadelphia:333-354 (also NASA TM 107623. NASA LaRC, 1992).

[25] Shivakumar KN, Allen HG, Avva VS (1994). Interlaminar tension strength of graphite/epoxy composite laminates. AIAA J;32(7):1478-1484.

[26] Jackson WJ, Ifju PG (1996). Through-the-thickness tensile strength of textile composites. In: Composite materials: Testing and design (Twelfth volume), ASTM STP1274, Eds: Deo RB, Saff CR. ASTM, Philadelphia:218-238.

[27] Pettersson KB (2005). The inclined double notch shear test for determination of interlaminar shear properties of composite laminates. PhD Thesis, Paper B. Department of Solid Mechanics, KTH, Stockholm.

[28] Ho H, Morton J, Farley GL (1994). Non-linear numerical analysis of the Iosipescu specimen for composite materials. Compos Sci Technol;50(3):355-365.

[29] Odegard G, Kumosa M (2000). Determination of shear strength of unidirectional composite materials with the Iosipescu and 10º off-axis shear tests. Compos Sci Techn;60(16):2917-2943.

[30] Pierron F (1998). Saint-Venant effects in the Iosipescu specimen. J Compos Mater; 32(22):1986-2015.

[31] Melin LN (2008). The modified Iosipescu shear test for orthotropic materials: Paper E. PhD Thesis. Royal Institute of Technology (KTH), Stockholm, Sweden.

[32] Neumeister J, Melin LN, (2003). A modified Iosipescu shear test for anisotropic composite materials. In: Proc 14th Int Conf on Composite Materials (ICCM-14) San Diego.

[33] Zhou G, Green ER, Morrison C (1995). In-plane and interlaminar shear properties of carbon/epoxy laminates. Compos Sci Techn;55(2):187-193.

[34] Oh JH, Kim JK, Lee DG, Jeong KS (1999). Interlaminar shear behavior of thick carbon/epoxy composite materials. J Compos Mater;33(22):2080-2115.

[35] Pettersson KB, Neumeister JM (2006). A tensile setup for the IDNS composite shear test. Composites Part A; 37(2):229-242.

[36] Melin LG et al. (2000). Evaluation of four composite shear test methods by digital speckle strain mapping and fractographic analysis. J Compos Technol Res;22(3)161-172.

[37] Hung S-C, Liechti KM (1997). An evaluation of the Arcan specimen for determining the shear moduli of fiber-reinforced composites. Exp Mech;37(4):460-468.

[38] Welsh JS, Adams DF (2000). Development of an electromechanical triaxial test facility for composite materials. Experimental Mechanics;40(3):312-320.

[39] Welsh JS, Adams DF (2001). Biaxial and triaxial failure strengths of 6061-T6 aluminium and AS4/3501-6 carbon/epoxy laminates obtained by testing thickness-tapered cruciform specimens. J Compos Technol Res;23(2):111-121.

[40] Collings TA (1974). Transverse compressive behaviour of unidirectional carbon fibre reinforced plastics. Composites;5(3):108-116.

[41] Henriksson A (1990). Transverse compressive behaviour of carbon-epoxy laminates and its influence of contact laws. FFA TN 1990-26. The Aeron. Res. Inst. of Sweden (FFA), Bromma.

Figure 1 *Transition from fully two-dimensional (a) to fully three-dimensional (c) stress states*

Figure 2 *Tubular specimens for (a) transverse normal/shear and (b) arbitrary biaxial loads*

[5] © Elsevier. Reproduced with permission.

Figure 3 *Typical cruciform specimen with reduced thickness gauge section*

Compiled from [7]. © Elsevier. Reproduced with permission.

Figure 4 *Cruciform specimen with four actuators (a) two actuators (b).*

[8] © Elsevier. Reproduced with permission.

Figure 5 *Strain states for axial loading of UD off-axis specimens*

Figure 6 *Strain states for axial loading of angle-ply specimens*

Figure 7 *Biaxial Arcan test with transverse stress in (a) tension and (b) compression*

[14] © SAMPE International. Reproduced with permission.

Figure 8 *Biaxial test with shear and transverse stress in (a) compression and (b) tension*

(a): [15] and (b): [16]. Both © Elsevier. Reproduced with permission.

Figure 9 *Interlaminar tensile test by (a) axial loading (b) flexure.*

[17] © Elsevier. Reproduced with permission

Figure 10 *The DERA specimen for through-thickness testing: (a) geometry of standard size specimen, (b) comparison of tensile (tabbed) and compressive specimens*

[19] © Elsevier. Reproduced with permission.

Figure 11 *Interlaminar tensile tests: a) Hinged loading; b) 4-Point-bend loading.*

[26] © ASTM International. Reproduced with permission.

Figure 12 *Stress distributions in the L-shaped flexural specimens.*

[26] © ASTM International. Reproduced with permission.

Figure 13 *Out-of-plane tensile strength of different material systems.*

[26] © ASTM International. Reproduced with permission.

Figure 14 *Geometry influence on interlaminar tensile strength.*

(σ_{2c} is in-plane tensile strength, σ_{3c} is out-of-plane tensile strength and r_i inner radius)

[24] © ASTM International. Reproduced with permission.

Figure 15 Geometry influence on ply thickness.

(r is radial position, r_i inner radius and t laminate thickness, c.f. Fig. 11a)

[24] © ASTM International. Reproduced with permission.

Figure 16 Tests for interlaminar shear strength: a) Iosipescu test, b) Short 3 Point Bend test, c) Double Notch Compression test, d) Inclined Double Notch Shear test, e) Inclined waisted specimen, f) Arcan specimen

Compiled from (a-d): [36] © ASTM. Reproduced with permission; (e): [20] © Maney Publishing. Reproduced with permission; (f): [13] © Elsevier. Reproduced with permission.

Table 1 Shear strengths from different tests. Data from [36].

	τ_{av}, [MPa]	$\tau_{\min}$, [MPa]	$\tau_{\max}$, [MPa]	Shear cusps
Iosipescu (90º) *	65	56	74	~50%
Iosipescu (0º) *, first peak	83	74	89	
Iosipescu (0º) *, maximum	114	107	122	
S3PB	133	129	137	67-72%
DNC	58	53	61	61-73%
IDNS	111	105	116	75-83%

* Note that definitions of fibre directions have been swapped to agree with ASTM D5379.

List of figures

Figure 1 Transition from fully two-dimensional (a) to fully three-dimensional (c) stress states

Figure 2 Tubular specimens for (a) transverse normal/shear and (b) arbitrary biaxial loads
[5] © Elsevier. Reproduced with permission.

Figure 3 Typical cruciform specimen with reduced thickness gauge section
Compiled from [7] © Elsevier. Reproduced with permission.

Figure 4 Cruciform specimen with four actuators (a) two actuators (b).
[8] © Elsevier. Reproduced with permission.

Figure 5 Strain states for axial loading of UD off-axis specimens

Figure 6 Strain states for axial loading of angle-ply specimens

Figure 7 Biaxial Arcan test with transverse stress in (a) tension and (b) compression
[14] © SAMPE International. Reproduced with permission.

Figure 8 Biaxial test with shear and transverse stress in (a) compression and (b) tension
(a): [15] and (b): [16]. Both © Elsevier. Reproduced with permission.

Figure 9 Interlaminar tensile test by (a) axial loading (b) flexure.
[17] © Elsevier. Reproduced with permission.

Figure 10 The DERA specimen for through-thickness testing: (a) geometry of standard size specimen, (b) comparison of tensile (tabbed) and compressive specimens
[19] © Elsevier. Reproduced with permission.

Figure 11 Interlaminar tensile tests: a) Hinged loading; b) 4-point-bend loading.
[26] © ASTM International. Reproduced with permission.

Figure 12 Stress distributions in the L-shaped flexural specimens.
[26] © ASTM International. Reproduced with permission.

Figure 13 Out-of-plane tensile strength of different material systems.
[26] © ASTM International. Reproduced with permission.

Figure 14 Geometry influence on interlaminar tensile strength.
(σ_{2c} is in-plane tensile strength, σ_{3c} is out-of-plane tensile strength and r_i inner radius)
[24] © ASTM International. Reproduced with permission.

Figure 15 Geometry influence on ply thickness.
(r is radial position, r_i inner radius and t laminate thickness, c.f. Fig. 11a)

[24] © ASTM International. Reproduced with permission.

Figure 16 Tests for interlaminar shear strength: a) Iosipescu test, b) Short 3 Point Bend test, c) Double Notch Compression test, d) Inclined Double Notch Shear test, e) Inclined waisted specimen, f) Arcan specimen
Compiled from (a-d): [36] © ASTM. Reproduced with permission; (e): [20]

© Maney Publishing. Reproduced with permission; (f): [13] © Elsevier.

Reproduced with permission.

Figure 17 Out-of-plane compression of constrained specimen

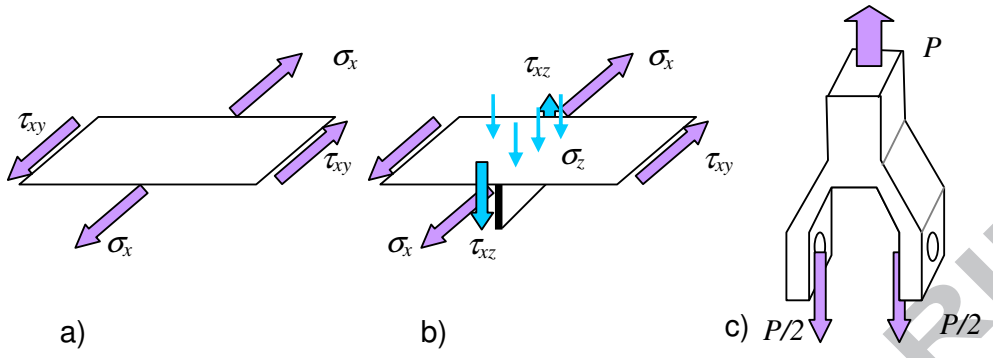

Figure 1 *Transition from fully two-dimensional (a) to fully three-dimensional (c) stress states*

Revision 1 submitted to Composites Science and Technology by Robin Olsson 24 Jan. 2011

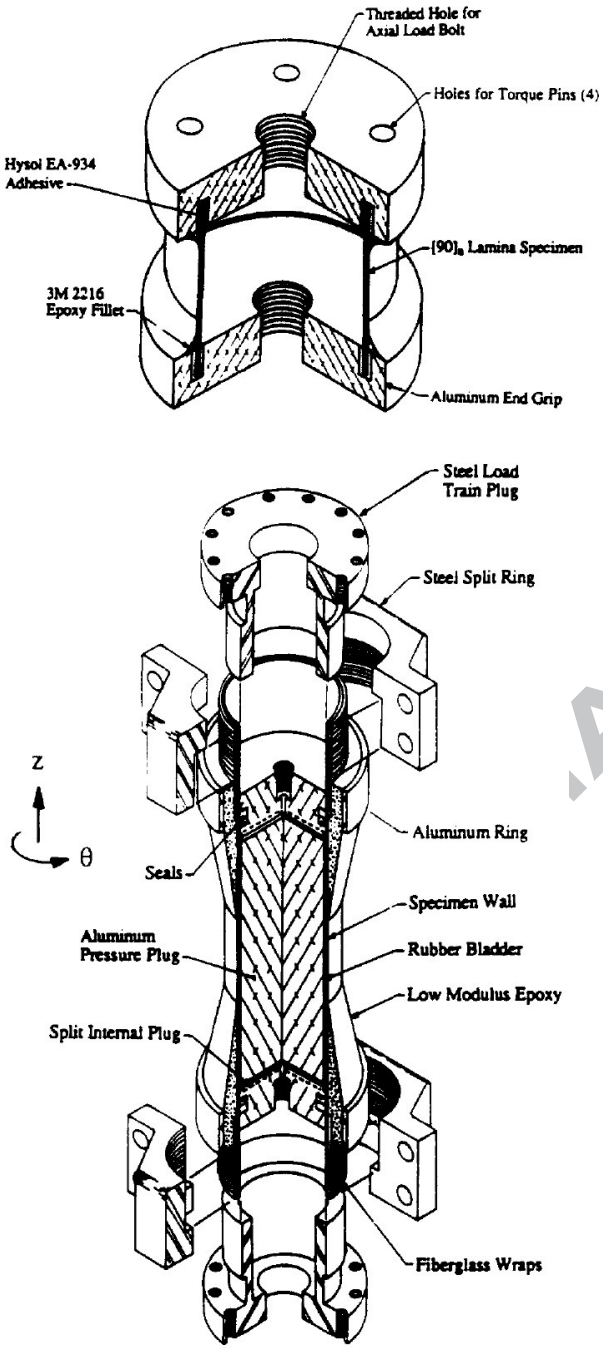

a) b)

Figure 2 Tubular specimens for (a) transverse normal/shear and (b) arbitrary biaxial loads

[5] © Elsevier. Reproduced with permission.

Revision 1 submitted to Composites Science and Technology by Robin Olsson 24 Jan. 2011

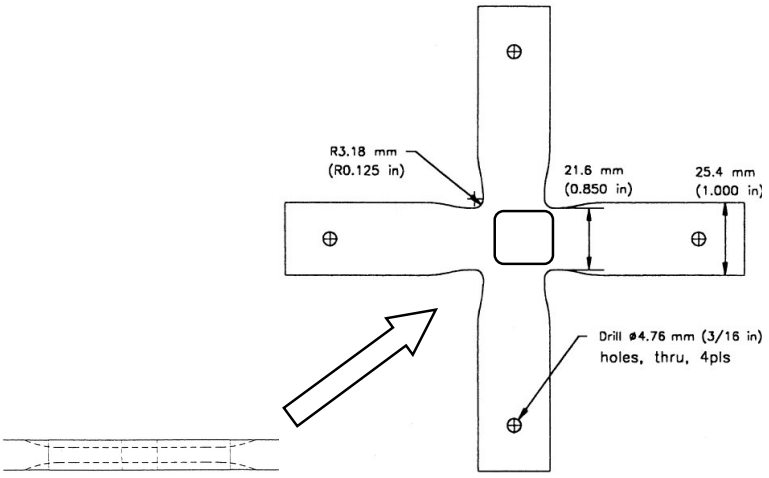

Figure 3 *Typical cruciform specimen with reduced thickness gauge section*

Compiled from [7]. © Elsevier. Reproduced with permission.

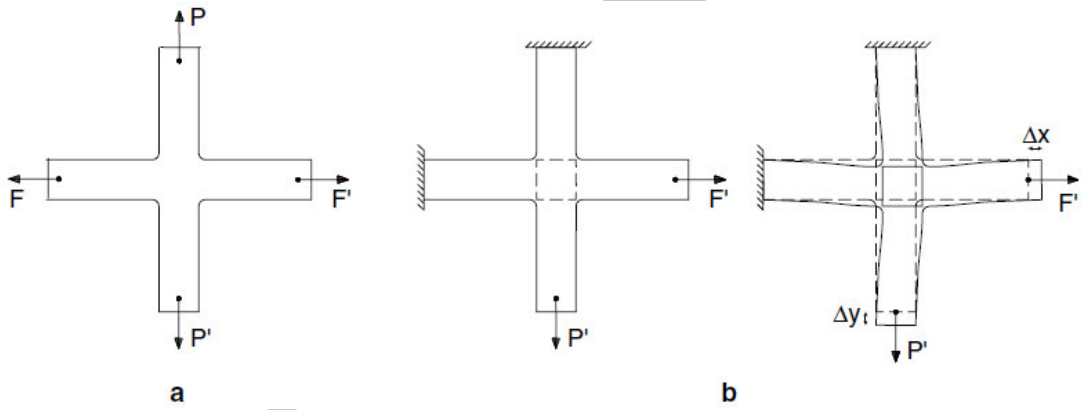

Figure 4 *Cruciform specimen with four actuators (a) two actuators (b).*

[8] © Elsevier. Reproduced with permission.

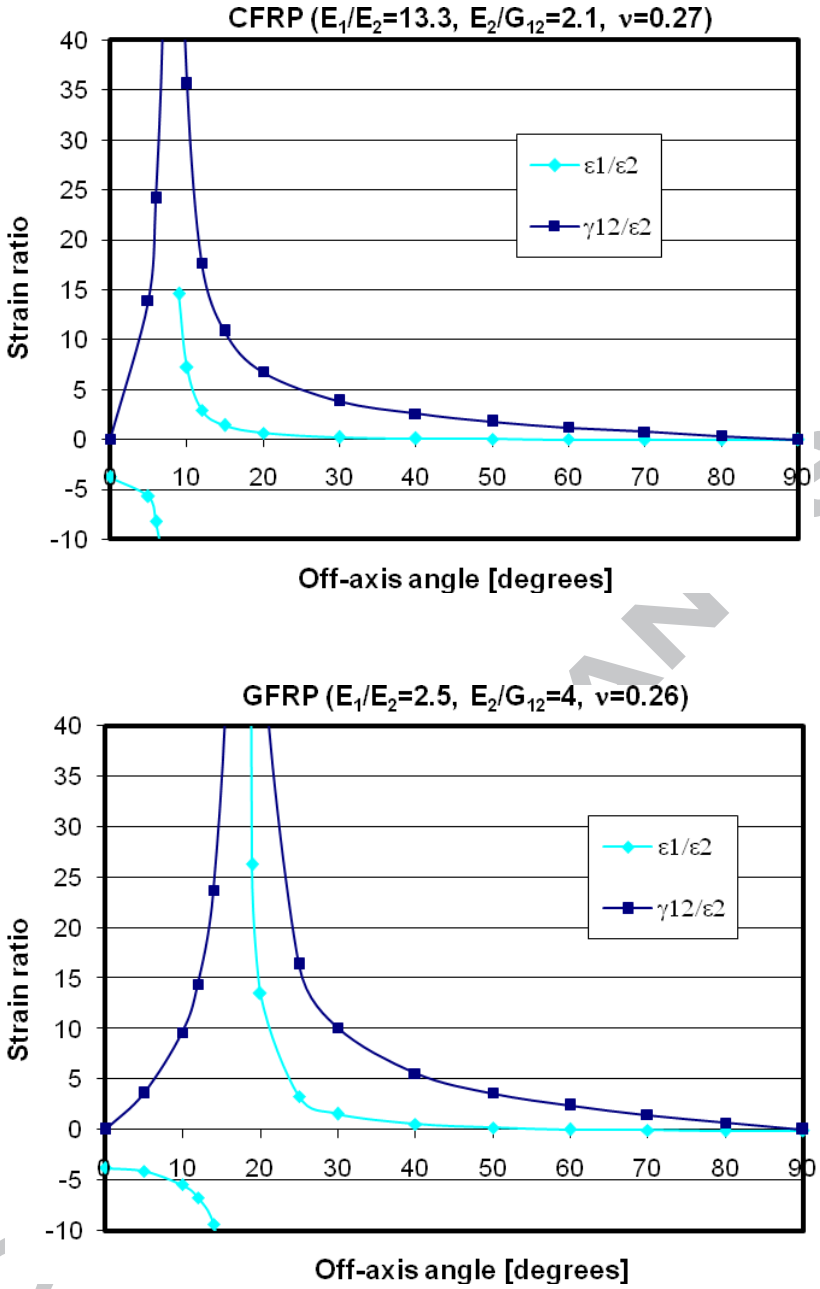

Figure 5 *Strain states for axial loading of UD off-axis specimens*

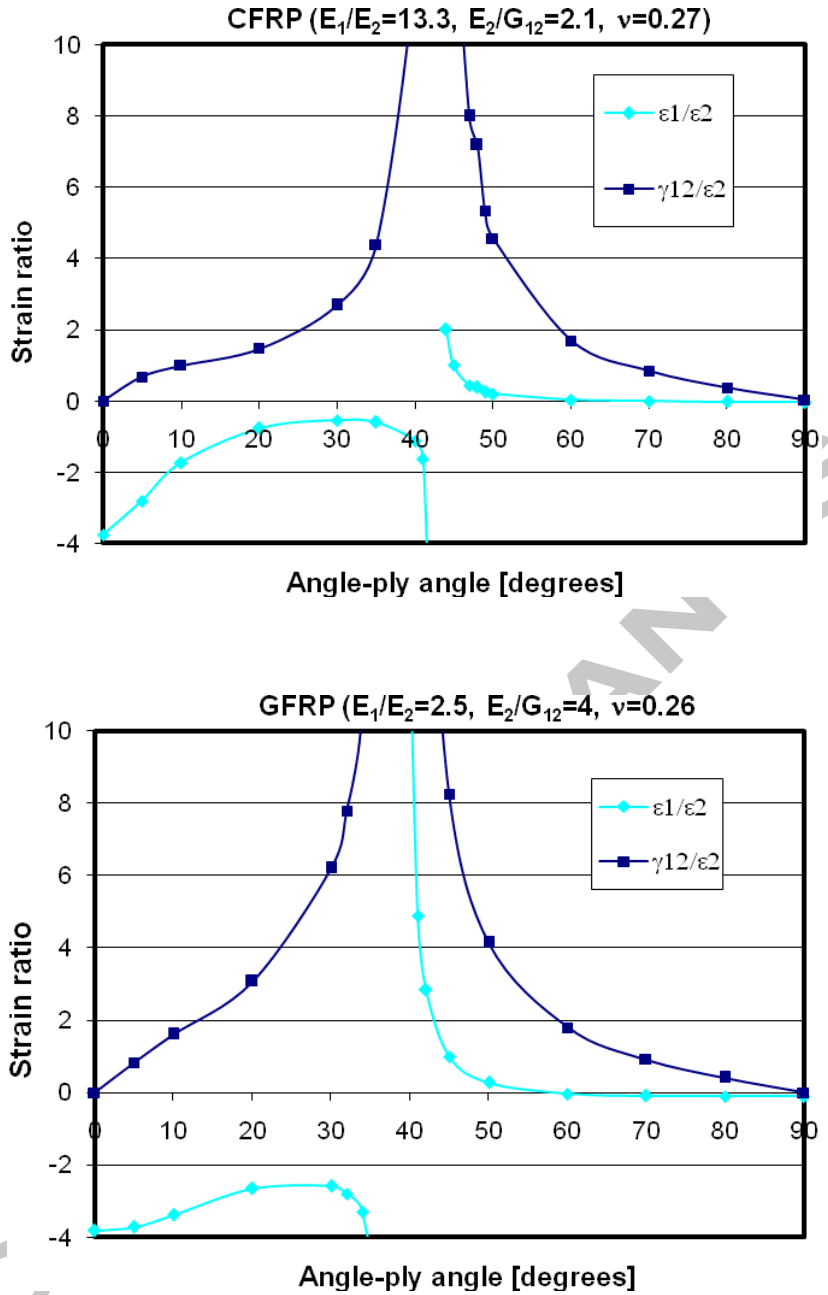

Figure 6 *Strain states for axial loading of angle-ply specimens*

Revision 1 submitted to Composites Science and Technology by Robin Olsson 24 Jan. 2011

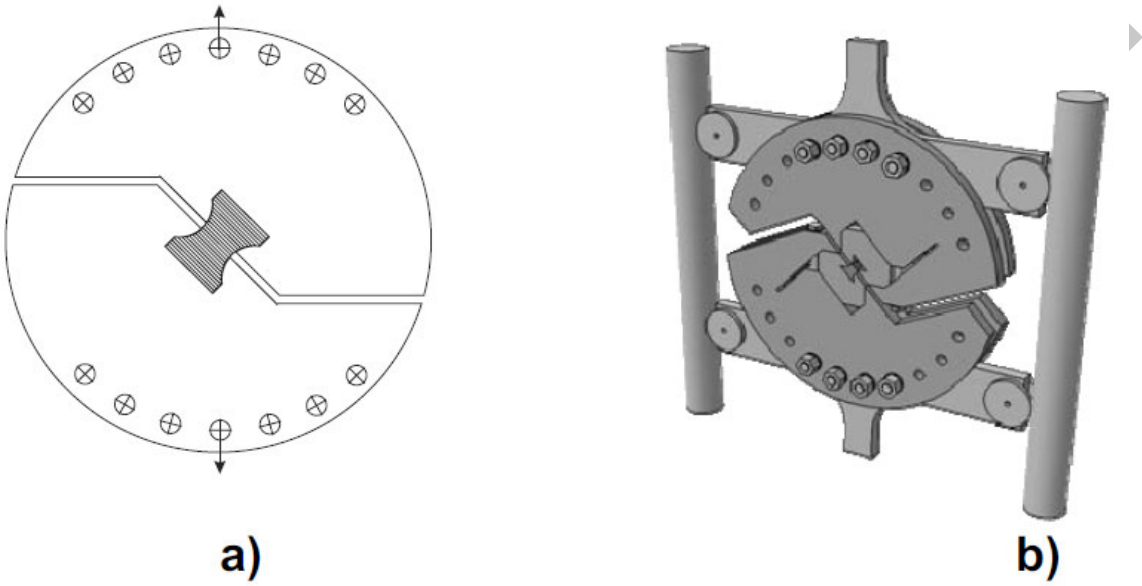

Figure 7 Biaxial Arcan test with transverse stress in (a) tension and (b) compression

[14] © SAMPE International. Reproduced with permission.

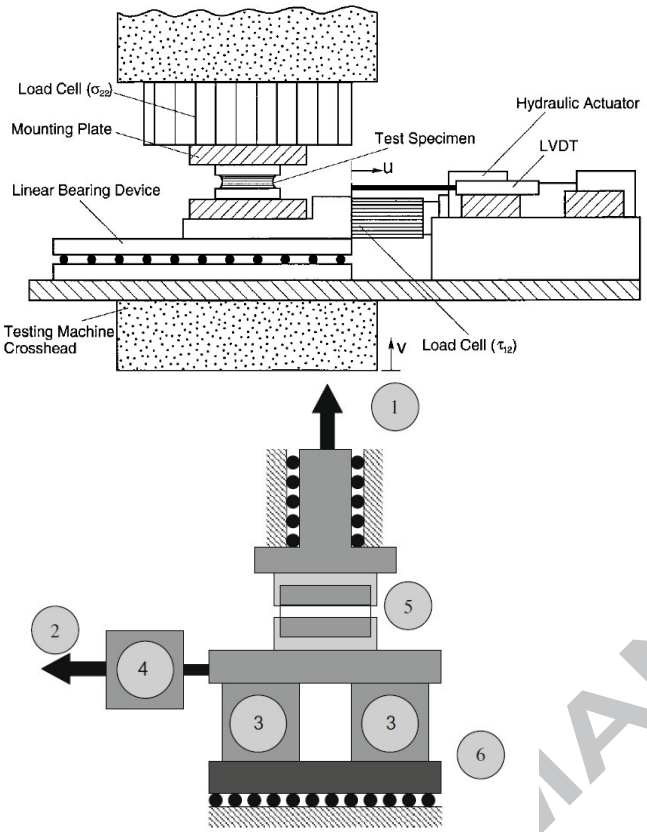

Dual actuator loading system: (1) vertical actuator; (2) horizontal actuator; (3) vertical load cells; (4) horizontal load cell; (5) specimen and grips; (6) sliding table assembly.

a) b)

Figure 8 Biaxial test with shear and transverse stress in (a) compression and (b) tension (a): [15] and (b): [16]. Both © Elsevier. Reproduced with permission.

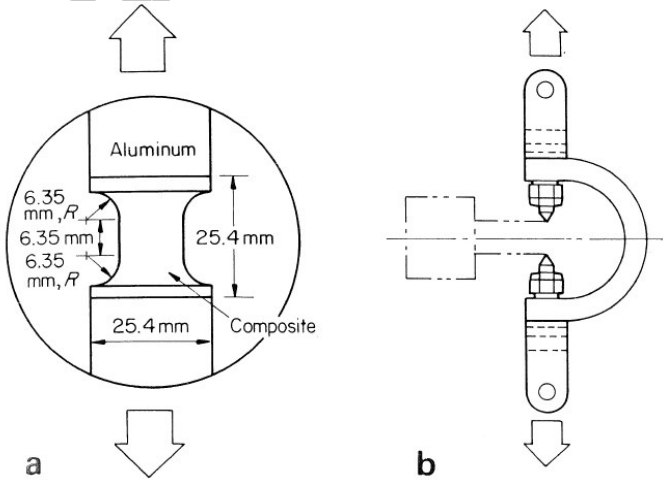

Figure 9 Interlaminar tensile test by (a) axial loading (b) flexure.

[17] © Elsevier. Reproduced with permission.

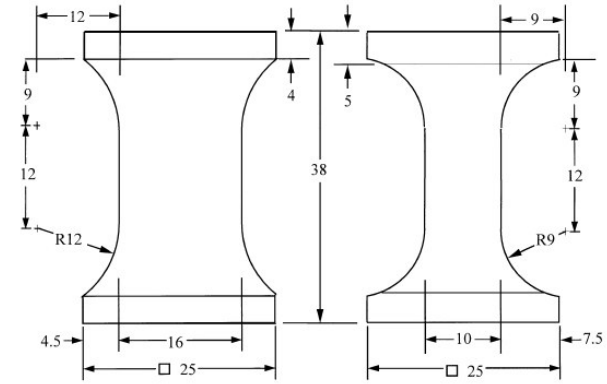

a) b)

Figure 10 The DERA specimen for through-thickness testing: (a) geometry of standard size specimen, (b) comparison of tensile (tabbed) and compressive specimens

[19] © Elsevier. Reproduced with permission.

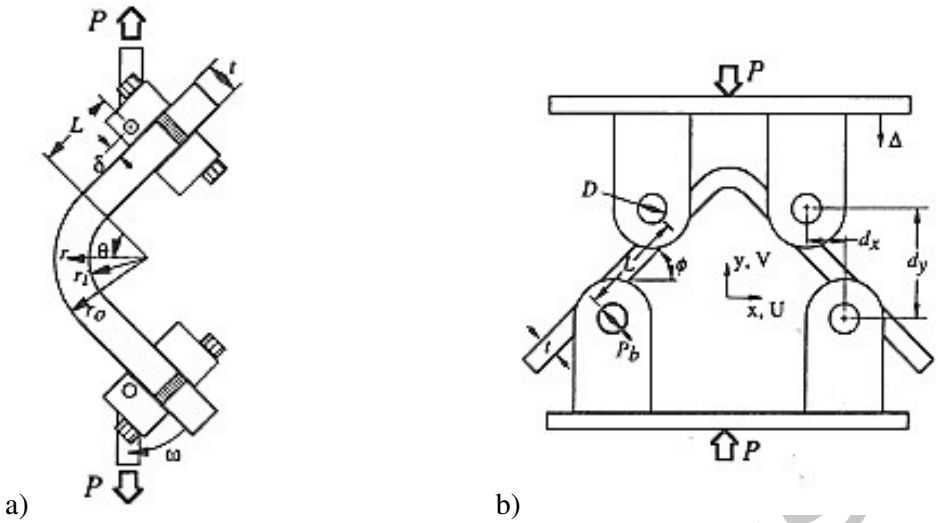

Figure 11 Interlaminar tensile tests: a) Hinged loading; b) 4-Point-bend loading .

[26] © ASTM International. Reproduced with permission.

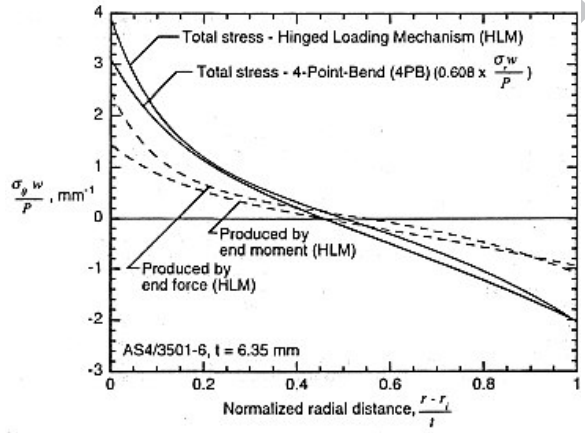

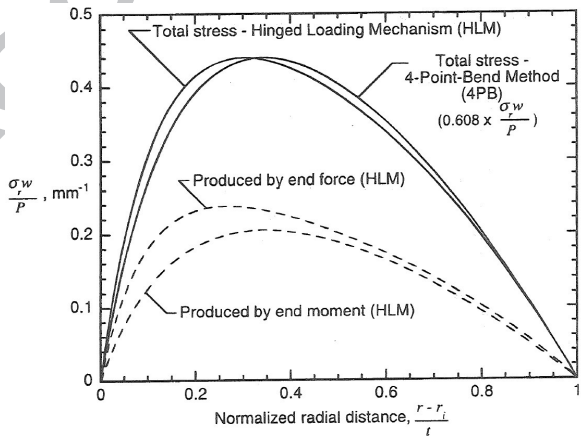

Figure 12 Stress distributions in the L-shaped flexural specimens

[26] © ASTM International. Reproduced with permission.

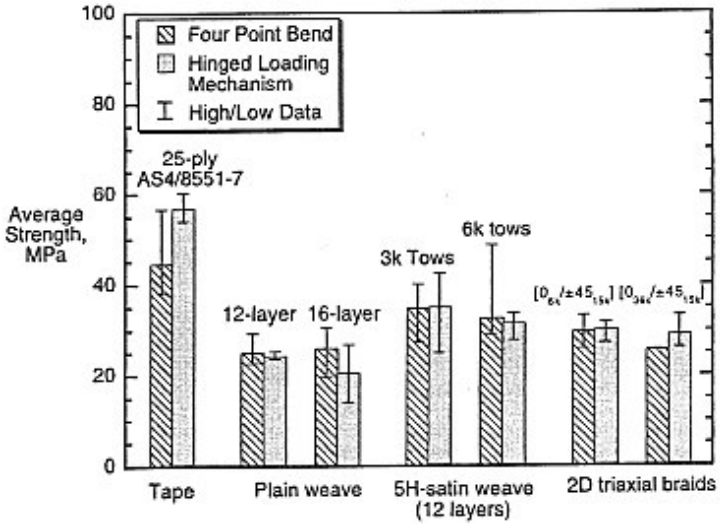

Figure 13 Out-of-plane tensile strength of different material systems.

[26] © ASTM International. Reproduced with permission.

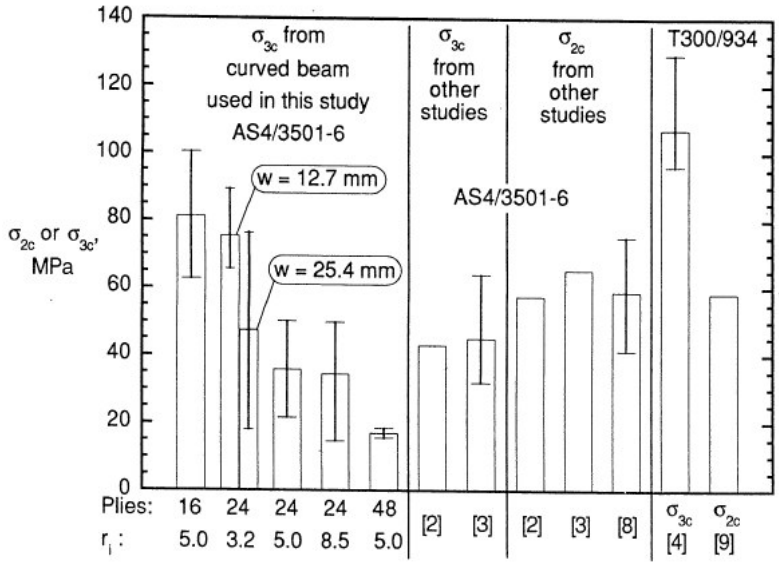

Figure 14 Geometry influence on transverse tensile strength.

(σ_{2c} is in-plane tensile strength, σ_{3c} is out-of-plane tensile strength and r_i inner radius)

[24] © ASTM International. Reproduced with permission.

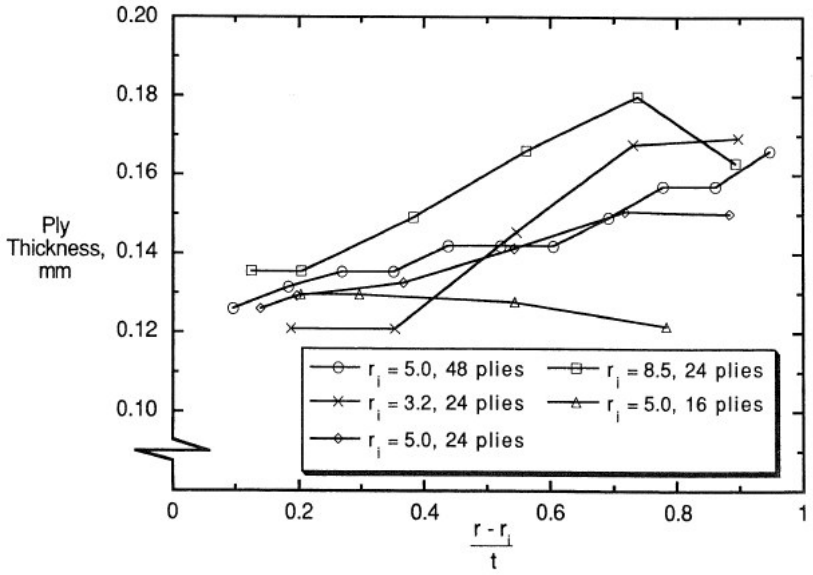

Figure 15 Influence of angle profile geometry on ply thickness.

(r is radial position, r_i inner radius and t laminate thickness, c.f. Fig. 11a)

[24] © ASTM International. Reproduced with permission.

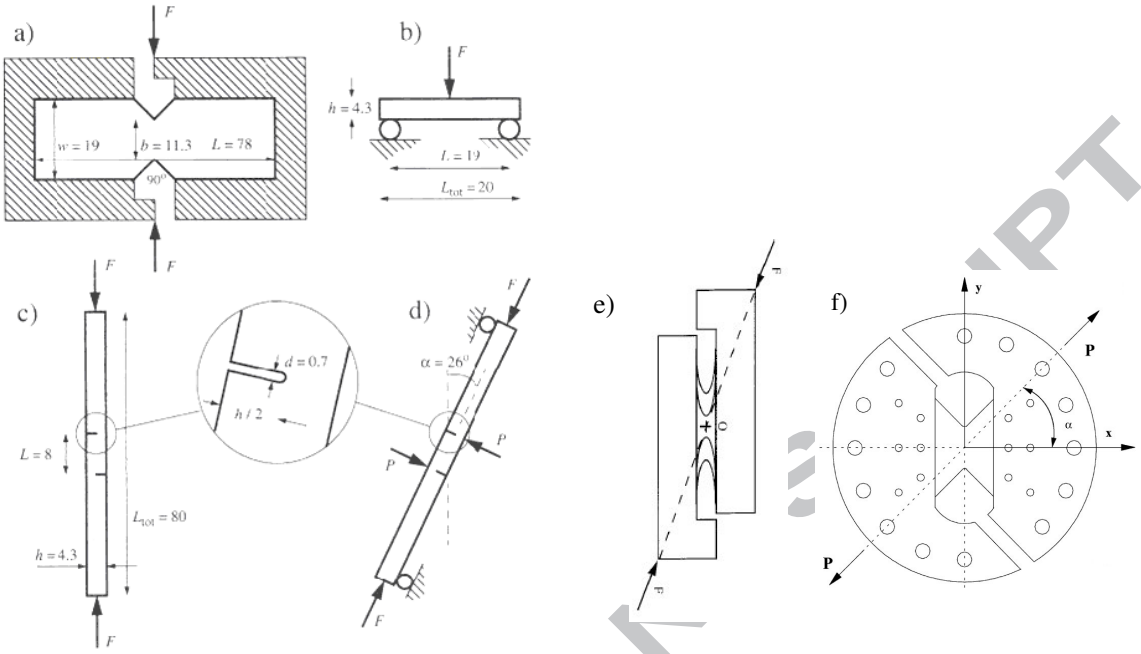

Figure 16 *Tests for interlaminar shear strength: a) Iosipescu test, b) Short 3 Point Bend test, c) Double Notch Compression test, d) Inclined Double Notch Shear test, e) Inclined waisted specimen, f) Arcan specimen*

Compiled from (a-d): [36] © ASTM. Reproduced with permission; (e): [20] © Maney Publishing. Reproduced with permission; (f): [13] © Elsevier. Reproduced with permission.

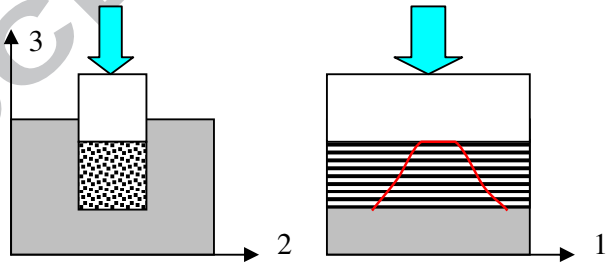

Figure 17 *Out-of-plane compression of constrained specimen*